Journal of the Georgian Geophysical Society,
Issue (B). , Physics of Atmosphere, Ocean and Space Plasma, v. 14, 2010, pp.161-182

On the convective motions in different layers of atmosphere

Anzor I. Gvelesiani

Iv. Javakhishvili Tbilisi State University, M. Nodia Institute of Geophysics
1, Alexidze Str., 0173 Tbilisi, Georgia, e-mail:
<anzor_gvelesiani@yahoo.com>

Abstract

From the unified point of view, this paper gives some known and new results of theoretical and experimental investigations of slow mesoscale convective motions in the neutral and conductive atmosphere. Specific thermo-hydrodynamic regime conditions of the considered mediums were taken into account for determination of onset of convection and the vertical velocity of arisen heat thermal. Carried out original analytical and numerical investigations showed that largescale eddy regions and zones of divergence and convergence responsible to existence of three-dimensional motions of air in the neutral atmosphere and in the ionosphere.

1. Introduction

It is common knowledge a lot of works devoted to the analytical theory of thermals beginning from the earliest works until now [1-16]. As is known, within a liquid or an atmosphere the heat heterogeneity causes both the Archimedes force and force of gravity's interaction. As a result of this interaction, with a beginning of turbulence when the Rayleigh number $Ra > 10^3$ within mentioned parts of mediums the warm bubbles begin their vertical motion and vibration because of origination and travel of the internal gravitational waves (here the Reynolds number $\mathrm{Re} \sim 0$; in the case of dynamical turbulence $\mathrm{Re} > 10^3$). For example for atmosphere the stability of a volume of finite sizes (in the present of horizontal contrasts) interchanging of heat and momentum with environment was considered by Priestley [8]. The criterion of Priestley up to a constant coincides with the Rayleigh number. It sets up correspondence between characteristics of the viable parcel and environment. More large volumes come into the state of instability at less temperatures, than small volumes, which quickly loose excess of their heat and are dragged because of the viscous resistance.

2. Mesoscale convective system (MCS) of clouds.

2.1. Some mechanisms of vertical motions: parcel lifting, layer lifting, and jet lifting.

2.1.1. Parcel lifting. For the troposphere very clear example are cumuliform clouds formed by penetrative convection. They represent warmed at the ground by sunshine air masses. Above the level of the cloud base the liberation of latent heat usually increases the buoyancy of the rising masses, which tower upwards in the form of great "bubbles" (known in the physics of clouds as thermals) having an upper surface which is roughly a spherical cap on whose outer parts there is vigorous mixing with the environment. The clouds grow upward until the ascending "bubbles" are completely eroded away by the mixing, or until their buoyancy is lost. In this case, from the equation of motion in the inviscid atmosphere for the vertical ve-

locity, w, of the thermals in the atmosphere the following well-known formulas were obtained by Exner [17, 18] ,

$$w = \left(2g \int_{z_1}^{z_2} \Delta T / T_e \, dz \right)^{1/2}, \qquad (1)$$

or

$$w = \left(2g \int_{z_1}^{z_2} \Delta \rho / \rho_e \, dz \right)^{1/2}, \qquad (2)$$

$$\frac{dw}{dt} = g \frac{\gamma - \gamma_d}{\gamma}, \quad z < z_c, \qquad (3)$$

where g is acceleration due to gravity; $\Delta T = T_i - T_e$, T_i and T_e are internal temperature of the thermal and external temperature of the air, γ is temperature gradient of the air, and γ_d is dry-adiabatic gradient of one, z_c is the condensation level, respectively. For the moist-adiabatic process above the condensation level the following formula is used:

$$\frac{dw}{dt} = g \frac{\gamma - \gamma_m}{\gamma}, \quad z > z_c, \qquad (4)$$

where γ_m is the temperature moist-adiabatic gradient of atmosphere.

The parcel lifting method considers only ascending motion of the air without of thermodynamical parameters of the atmosphere cause by the descending motion of the cold air.

Firstly, the convective vertical velocity of the air in cloud taking into consideration the descending motion of the cold air was realized by the Shishkin layer lifting method [19, 20]):

$$w = \left(\int_{z_0}^{z} \frac{2c_p q}{A(1-q)} [\{\gamma - \gamma_m\} - q(\gamma_d - \gamma_m)] dz \right)^{1/2}, \qquad (5)$$

where c_p is the specific heat of dry air at constant pressure, q is relative content of water in the layer of atmosphere A is the mechanical equivalent of heat (0.24 cal/erg).

Comparison of ascending velocity calculated by the parcel view of lifting and by the layer one shows the curves $w(z)$ diverge and differ qualitatively character: after the level of maximum of velocity the first curve continuously increases but second one, vice versa, continuously decreases. So far the Shishkin method (of layer lifting) as the practice of observations on convective clouds showed its accuracy. Note that some other theoretical and numerical solutions of the thermohydrodynamical equations system (even non-linear ones, too) use this method result as a test for comparison.

Considering the thermal lifting as the solid sphere motion and taking into account the air resistance, the author of report [21] gives the equation of motion in the form.

$$\frac{dw}{dt} \approx g \frac{\Delta T}{T} - C_D \frac{w^2}{R}, \qquad (6)$$

where R is radius of the thermal, ΔT is the temperature drop between thermal temperature, T', and the surrounding air temperature, T. For linear exchange of the temperature and thermal radius with z, the solution of equation (6) is:

$$w = \left\{ \left[w_0 + \int_{z_0}^{z} \frac{\Delta T_0 + \Delta\gamma}{T_0 - \gamma z} \left(\frac{R_0 + \gamma_R z}{R_0 + \gamma_R z_0} \right)^{C/\gamma_R} dz \right] \left(\frac{R_0 + \gamma_R z_0}{R_0 + \gamma_R z} \right)^{C/\gamma_R} \right\}^{1/2}, \qquad (7)$$

where $\gamma = -dT/dz$, $\Delta\gamma = \gamma' - \gamma$, $\gamma' = -dT'/dz$, $\gamma_R = dR/dz$, the subindex 0 corresponds to the base of thermal. Naturally, the calculations must provide layer-by-layer. Calculations of conditions of instability by parcel, layer, and suggested lifting methods show that both the first and second methods give non-real result: the adiabatic vertical velocity grows with height. Whereas according (7) and the aerological diagram the condensation level and velocity of ascending air may be determined. Comparison results of upper boundary clouds obtained by mentioned methods show that suggested method gives better accordance with radar observations than other abovementioned methods (see also results of [29]).

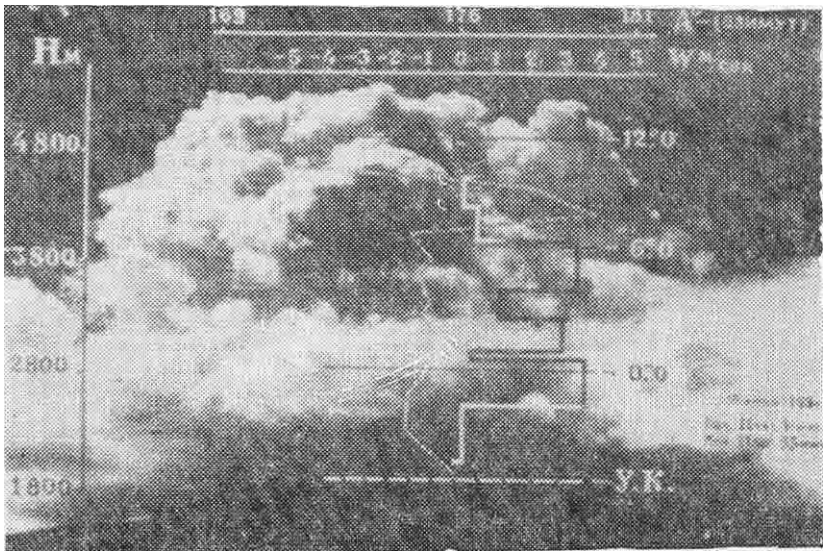

Fig. 1. The velocity profile of ascending air inside the deep cumulus cloud (above Telavis-Tsivi m., Alazany Valley, Georgia, June 16, 1962, photographed from Ruispiri v.) [22, 23].

A pilot-balloon (PB) with angled reflector was used for observation of its motion inside the towering cumulus cloud by radar technique. Fig. 1 shows the trajectory of PB indicated by firm heavy line, and the vertical profile velocities of PB (ascending air) numerically calculated using (7) – by the dashed line). It is seen very well as "lucky" parcel rises from below cloud base to the upper boundary of the cloud in the natural conditions. This picture confirms a tradition commonly held view vertical motion of bubbles or parcels of warm, moist air originating in the boundary layer, accelerating upward after being forced above the local level of free convection, entraining varying amounts of environmental air via in-cloud turbulence as they rise, then decelerating and eventually stopping and spreading out laterally at or near a level of neutral buoyancy (see also [15]). According to observations in Alazany Valley (from Ruispiri v.) the maximal velocity of vertical motion of the cloud top in most cases changes in interval 3-15 m/s, and, as a whole, taking into account all cases of the observations in 1-18 m/s [24] (compare with Fig. 6, Fig. 3a,b). More detail, the cloud top velocities was changed from

(a) in initial stage of evolution when $h_{\max} = 4.5$ km,

$$\overline{w}_{min} = 0.6 \text{ to } \overline{w}_{max} = 2.8 \text{ m/s, at } w_{max} = 6.7 \text{ m/s};$$

(b) in middle stage of evolution when $h_{\max} \approx 7.0$ km,

$\overline{w}_{min} = 0.7$ to $\overline{w}_{max} = 4.8$ m/s, at $w_{max} = 13.1$ m/s;

(c) in mature stage of evolution when $h_{\max} > 7.0$ km,

$\overline{w}_{min} = 0.5$ to $\overline{w}_{max} = 7.9$ m/s, $v_{\max}$ m/s = 13.1 m/s

Declining of the cloud top velocities changed

(a) in initial stage of evolution from

$\overline{w}_{min} = -0.5$ to $\overline{w}_{max} = -6.2$ m/s, at $w_{max} = -14.1$ m/s

(b) in mature stage of evolution from

$\overline{w}_{min} = -0.5$ to $\overline{w}_{max} = -7.0$ m/s, at $w_{max} = -16.6$ m/s

(c) in middle stage of evolution from

$\overline{w}_{min} = -0.7$ to $\overline{w}_{max} = -7.7$ m/s, at $w_{max} = -15.0$ m/s.

The declining of the velocities may be caused by erosion of thermals or variability of temperature stratification in the cloud (see Fig. 1 and Fig. 2, where parcels rising from below cloud base, may entrain environmental air from some level, lose buoyancy, and decelerate accordingly).

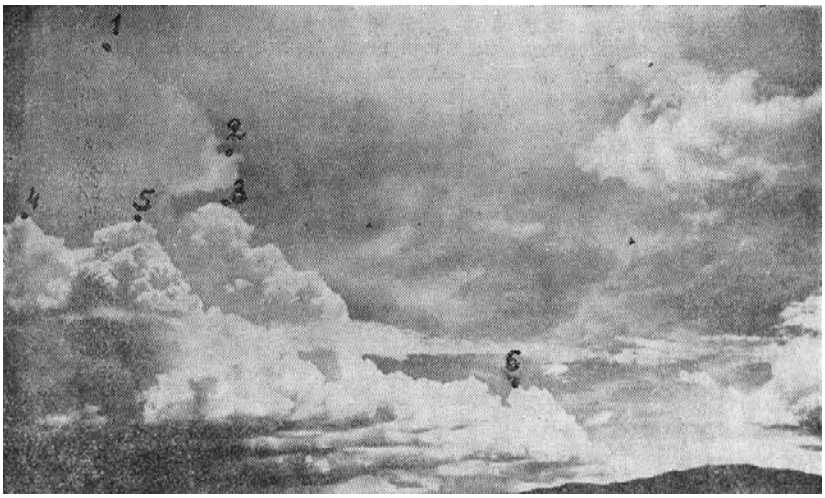

Fig. 2. Stereopicture of the bank of cumulus with numerated "lucky"thermals which achieved the top of cloud (above Tsivi-Gombori m. r., Alazany Valley, Georgia, June 6, 1961, photographed from Napareuli v.) [25].

See, also, the work [15] which shows a schematic picture of evolution entraining air parcels in a cumulus. The cumulus cloud composed of entraining air parcels is following: as parcels rise from below cloud base, they may entrain environmental air from some level, lose buoyancy, and decelerate accordingly. "Lucky" parcels experience no entrainment and rise undiluted to the entrainment's level of zero buoyancy, i.e. upper boundary of the cloud.

2.2. Layer lifting. This traditional view considers the upward air motion maintaining a mature mesoscale convective system to occur in the form of a deep slantwise ascending layer of air.

In the case of parcel lifting it moves in a rest atmosphere. But in real atmosphere the motion of individual particle gives rise to compensation flow in the surrounding atmosphere at once, and, therefore, a state change. Thus, individual parcel will rise when surrounded by downstream state of which changes. Typical and most significant example of this process is evolution of cumulus when moist-adiabatically developing cumulus rises in a dry-adiabatically falling blast.

The layer lifting is based on the following assumptions [26]:

(a) some horizontally infinite isobaric layer contains ascending and descending flows of air in its boundaries, i.e.

$$\int_{S'} \rho' w' \, ds' = \int_{S} \rho w \, ds \,, \quad \text{or} \quad M' w' = -Mw, \tag{8}$$

where in the first equality S', ρ', w', and M', are the area, density, vertical velocity, and mass of ascending air, respectively, and S, ρ, w, and M are the area, density, vertical velocity, and mass of descending air, respectively; in the second one w' and w are mean velocities of the ascending and descending air flows, respectively;

(b) at initial time the air is rest and field of mass is uniform and barotropic (isobaric and isosteric surfaces coincide);

(c) change of state is adiabatic, i.e. local changes of temperature inside the layer occur by convection of the air mass having different temperature; following relations take place there: $\partial T'/\partial t = w'(\gamma - \gamma_a)$ in ascending unsaturated air, $\partial T'/\partial t = w'(\gamma - \gamma'_a)$ in ascending saturated air, $\partial T/\partial t = w(\gamma - \gamma_a)$ in descending unsaturated air, $\partial T/\partial t = w(\gamma - \gamma'_a)$ in descending saturated air.

Then a heat accumulated inside of the layer in a unite of time connected with local changing of temperature equals to

$$\frac{\partial Q}{\partial t} = c_P \left(M \frac{\partial T}{\partial t} + M' \frac{\partial T'}{\partial t} \right) = c_P (M + M') \frac{\partial T}{\partial t} + c_P M' \left(\frac{\partial T'}{\partial t} - \frac{\partial T}{\partial t} \right). \tag{9}$$

It is evident that last member of this expression is equal to the heat which is transformed into kinetic energy of the air.

Well-known three cases of the air ascending through the descending air are, respectively: (a) unsaturated air, (b) saturated air, (c) moist-adiabatically air lifting through the surrounding dry-adiabatically descending air.

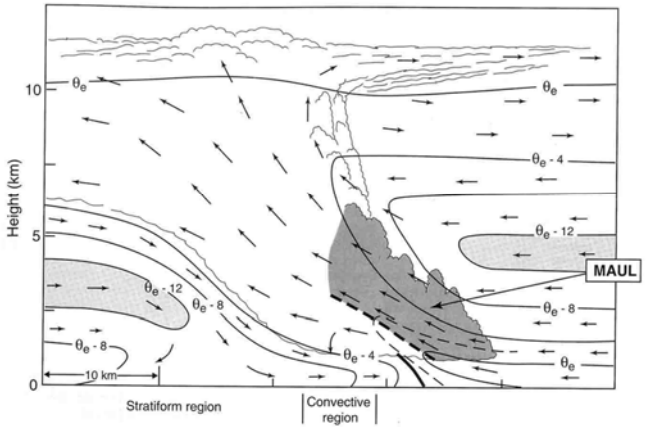

Fig. 3a. Idealized cross section through slab convective overturning (Bryan, Fritsch (2003) [15]).

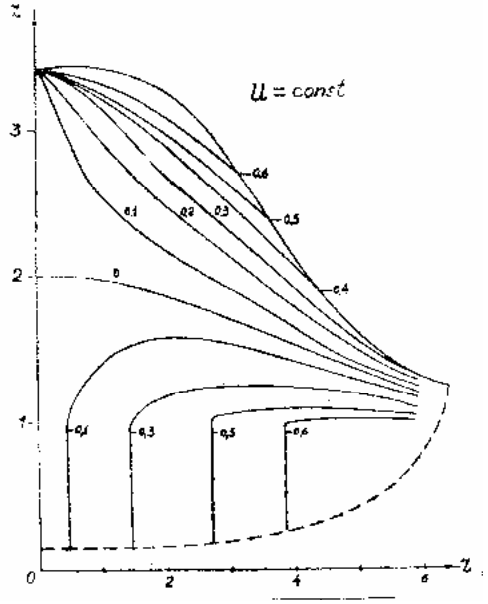

Fig. 3b. Gutman's axisymmetic cumulus model (1962)[30].

In Fig. 3a, the flow vectors are system-relative, scalloped lines indicate cloud boundaries, solid lines – θ_e contours every 4K (thin dashed line – an intermediate contour, bold dashed line – axis of highest values), bold solid line – outflow zone, light shading highlights

middle level layer of low-θ_e air, and dark shading depicts the moist absolutely unstable layer [15]. As is seen, this picture (Fig. 3a) is similar to Gutman's theoretical model constructed firstly more than four decade earlier (Fig. 3b).

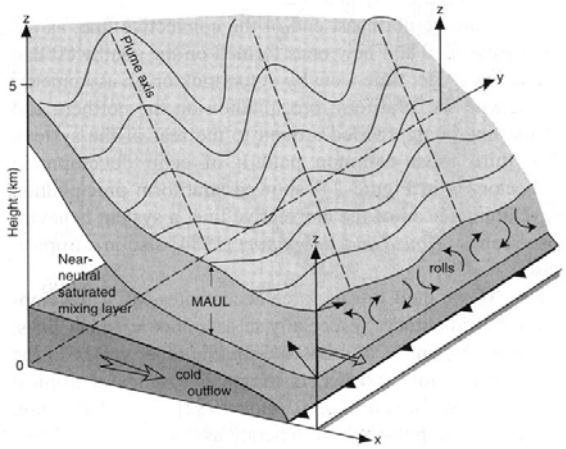

Fig. 4. Schematic of rolls in the convective region of an MCS
(Bryan, Fritsch (2003) [15].

According to a numerical model [27].with extremely high resolution the cells may have a lateral component of circulation in which the buoyancy elements overturn in rolls aligned along the shear within the overturning layer. Fig. 4 indicates the geometry of the rolls. These elongated cells would appear to explain the common observation of cigar-shaped cells oriented at an oblique angle to the line of cells in squall line MCSs.

In Fig. 4, bold solid arrows at the top and bottom of the MAUL (moist absolutely unstable layer) indicate the ground-relative wind flow. The double-line arrow indicates the shear vector. In this schematic the plumes axes are not perpendicular to the surface gust front (as they are in the numerical simulation). Note the shear vector may not be perpendicular to the gust front [27]).

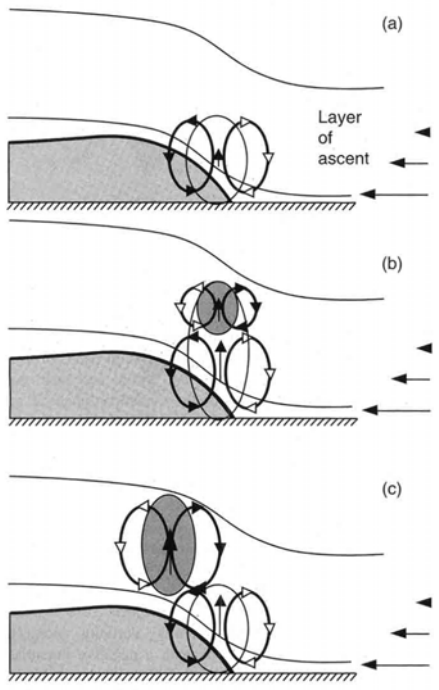

Fig. 5. Interpretation of an updraft cell (open oval) in the convective region
of an MCS as a buoyancy element. [15]

According to radar observations convective regions have cores of maximum reflectivity, stratiform regions are centered in the areas of medium intensity echo with no maximum reflectivity cores.

Fig 5 shows: (a) circulation tendency at the nose of the cold pool (shaded); (b) positively buoyant region (shaded oval) with associated circulation tendency forced by perturbation pressure field; (c) same as (b) but a later time.

Below, Fig. 6 shows typical characteristics of convective motions in an MCS. The numbers (from bottom to top) indicate the observed ranges of values of the depth of the inflow layer, horizontal relative velocity of inflow and outflow air currents, the slope of the updraft (angle measured relative to the ocean surface), and the width of the divergent region aloft. The horizontal directional differences of the low level updraft inflow and middle level downdraft inflow were often significantly different from 180°.

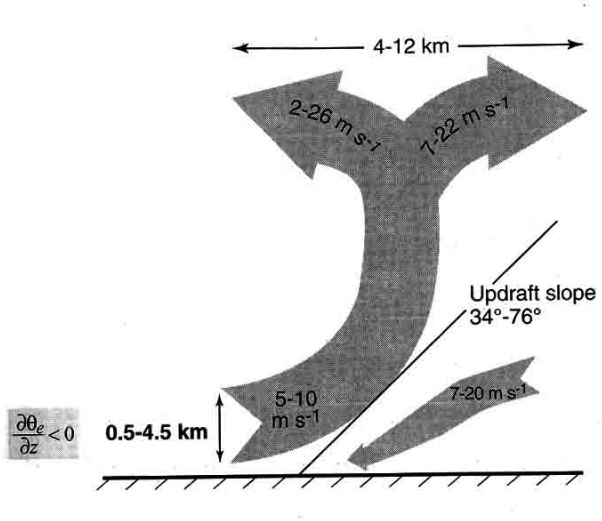

Fig. 6. Schematic of airflow in the convective regions of an MCS over the western Pacific as observed by airborne Doppler radar. [15].

The updrafts were nearly always slantwise and consisted of finite layers of air rising over an apparent downdraft cold pool. The layer of air composing the sloping updraft ranged from 0.5 to 4.5 km in depth, notably deeper than the planetary boundary layer. This layer of air was potentially unstable ($\partial\theta_e / \partial z < 0$) but, none the less, maintained a well-defined layered structure in radar radial data.

2.3. Jet lifting. Condensation "torchs" generating within the vertical jet of moist air are considered in [28] as a model of convective/cumulus cloud. The vertical profiles of temperature, velocity, and humidity and a trajectory of the jet were calculated on the basis of four differential equations. Main differential equations system when horizontal wind velocity $v = 0$ is following

$$\frac{2}{R}\frac{dR}{dz} = \frac{C}{R}\frac{T'}{T} - \frac{1}{w}\frac{dw}{dz} + \frac{1}{T'}\frac{dT'}{dz} + \frac{Mg}{NkT}, \qquad \frac{1}{w}\frac{dw}{dz} = \frac{g}{w^2}\frac{T'-T}{T} - \frac{C}{R}\frac{T'}{T},$$
$$-\frac{1}{T'}\frac{dT'}{dz} = \frac{C}{R}\frac{T'-T}{T} + \frac{g}{c'_p T}, \quad \frac{df'}{dz} = -f'\left[\left(1-\frac{fE}{f'E'}\right)\frac{C}{R}\frac{T'}{T}\right] + \frac{1}{kT'^2}\frac{dT'}{dz} + \frac{Mg}{NkT}; \qquad (10)\text{-}(13)$$

instead of equation (11), above the level of condensation the equation of jet temperature takes the form:

$$-\frac{dT'}{dz}=\left\{\frac{C}{R}\frac{T'}{T}\left[\frac{\mu}{M}\frac{1}{c'_p p}(E'-fE)+(T'-T)\right]+\frac{\mu E' gL}{NkTc'_p p}+\frac{g}{c'_p}\frac{T'}{T}\right\}\left(1+\frac{\mu L^2 E'}{kT'^2 Mc'_p p}\right)^{-1}, \quad (14)$$

where R is the radius of the jet, C is a constant of air entrainment in the jet, w is the velocity of jet along its axis, z is vertical axis of the co-ordinates; g – is the acceleration of gravity, T' and T is the temperature of the jet and atmosphere, respectively, M is the molecular weight of air, N is the Avogadro number, k is the Boltzmann constant; f' and f is relative humidity of the jet and atmosphere, E' and E is absolute humidity of the jet and atmosphere, respectively, μ is the molecular weight of the water vapour, p is the atmosphere pressure, L is the evaporation heat; c'_p is the specific heat of the air of the jet at constant pressure.

Assumed that $L=0$ or E' and $E=0$ in equation (12), we return to the equation for "dry" jet (11). Note also, that instead of equation (10) one can use the equation for relative content of the water vapour q' in the jet (and q – in the atmosphere):

$$-\frac{1}{q'-q}\frac{dq'}{dz}=\frac{C}{R}\frac{T'}{T}. \quad (15)$$

Taking into account the horizontal velocity of the wind, v, (drift of the jet by the wind) the value C/R in equations (11)-(14) must be replaced (except for (8), for simplification of the calculations, without great error) by the expression $CR^{-1}[1+(v/w)^2]^{1/2}$:

Results of the jet parameters calculations on the basis of equations (10)-(14) and the correction (10) are represented in Fig. 7a. [28] As evident from Fig. 8a, the jet consists of three ranges: active, intermediate, and passive (w = 0).

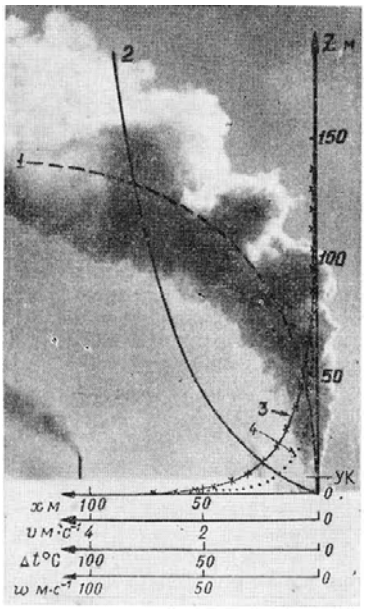

(a)

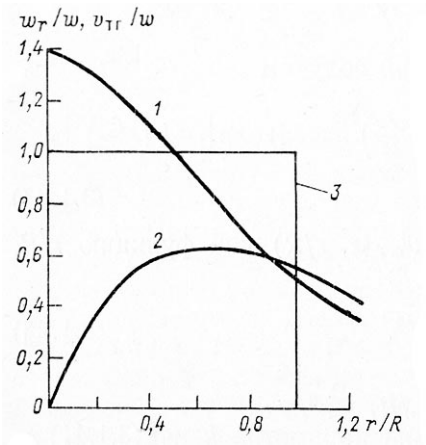

(b)

Fig.7. (**a**): (1) – trajectory of the jet centre, $X(z)$; (2) – profile of the wind velocity (measured), $v(z)$; (3) – excess of air temperature relative to environment along the jet axis, $\Delta T(z)$; (4) – calculated vertical velocity of the wind, $w(z)$; (УК) is the level of condensation;
(**b**): typical radial profile of the jet velocities: (1) – vertical component, $w_r(z, r/R)$; (2) – horizontal component, $v_r(z, r/R)$; Π-type profile of vertical component.

Considering the model of the jet with parameterized radial distribution of its meteovalues, for vertical velocity is written the approximation

$$w_r(z,r/R) = Aw(z)\exp[-k(r/R)^n], \qquad A = \frac{w_{r_{\max}}(z,0)}{w(z)} = \frac{R}{r_m}\sqrt{\frac{n}{2\Gamma(2/n)}}, \qquad (16)$$

where r is a variable radius, $R = R(z)$ is a radius of the jet with a Π- type profile of the jet meteovalues, A, k, and n are parameters, controlled by some correct assumptions on the basis of experimental data. From the right it is given the value of A (for $r/R = 0$) equal the relation of the maximal (in the center of the jet) vertical velocity, $w_{r_{\max}}(z,0)$ to the mean value of the Π-type profile velocity $w(z)$. On the basis of (14) and the experimental data $4/3 \le A \le 7/4$, $r_m/R =$ 0.64, n = 4, and k = 3, i.e., $w_r(z,r/R) = 1.6\sqrt{2\Gamma(1/2)}w(z)\exp[-3(r/R)^4]$, typical profiles of the air jet velocities were calculated and given in graphic form.

Shown in the Fig. 7 the vertical velocity of the hot submerged air jet, *w,* (when at the nozzle of the turbo-jet engine $w_0 = 34\,m\cdot s^{-1}$, $R_0 = 1.6\,m$, $\Delta T_0 = 63^0 C$) is a function of the jet radius and equals to $\frac{w^2}{R} = \frac{g}{C} \approx 50\,m\cdot s^{-2}$, $C = 0.18 \div 0.25$.

Fig. 8 shows results of numerical calculations of model convective cloud on the basis of radiosounding and ring chart data of Ruispiri village weather station for the territory of the Alazani Valley (Georgia), 29 June 1969 [29].

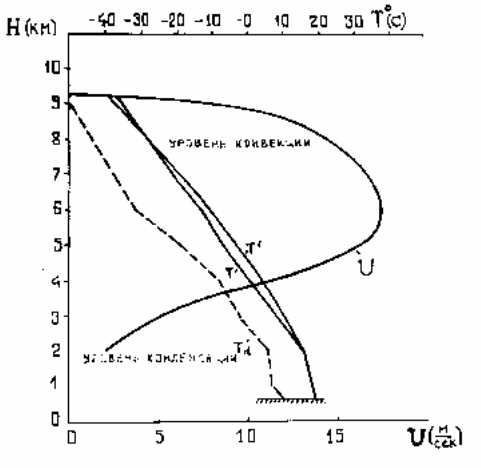

Fig. 8. (1) Profile of the upstream velocity w (here U), (m/s), dew point, $T_d(z)$, air temperature inside of the cloud, $T'(z)$, air temperature outside of the cloud, $T(z)$. [29]

There are given a stratification of the atmosphere $T(z)$, dew point, $T_d(z)$, air temperature inside of the cloud, $T'(z)$ the upstream velocity inside of the cloud, w, (m/s). Maximal height of cloud was $H_m = 9.8\,km$ above sea level, maximal value of the upstream velocity inside of cloud,

$$w_m = 14.2\,m/s.$$

2.4.1. Axisymmetric cumulus. Here only results of are considered where approximate nonlinear theory of a stationary cumulus cloud is given. Simplified system of equations of the stationary axisymmetric cumulus cloud has following dimensionless form [12]:

$$u\frac{\partial u}{\partial r}+w\frac{\partial u}{\partial z}=-\frac{\partial \pi}{\partial r}+\frac{\partial}{\partial r}\left(\frac{1}{r}\frac{\partial (ur)}{\partial r}\right)+\varepsilon\frac{\partial^2 u}{\partial z^2},$$

$$u\frac{\partial w}{\partial r}+w\frac{\partial w}{\partial z}=-\varepsilon\frac{\partial \pi}{\partial z}+\vartheta+\frac{1}{r}\frac{\partial}{\partial r}\left(r\frac{\partial w}{\partial r}\right)+\varepsilon\frac{\partial w}{\partial z^2},\ u\frac{\partial \vartheta}{\partial r}+w\frac{\partial \vartheta}{\partial z}=\pm w+\frac{1}{r}\frac{\partial}{\partial r}\left(r\frac{\partial \vartheta}{\partial r}\right)+\varepsilon\frac{\partial^2 \vartheta}{\partial z^2},$$

$$\frac{\partial ur}{\partial r}+\frac{\partial wr}{\partial z}=0, \qquad (17)$$

and the boundary conditions are, respectively,

$$w=\vartheta=0 \text{ at } z=0;\ u=\frac{\partial \vartheta}{\partial r}=\frac{\partial w}{\partial r}=0 \text{ at } r=0;\ w=\vartheta=0 \text{ at } r=\infty;\ \int_0 wrdr<\infty. \qquad (18)$$

The system of equations (17) with the boundary conditions (18) has an unambiguous solution describing the cumulus cloud. It is necessary to note that taking into account evaporation and turbulence processes the discontinuous jumps of the cloud parameters will be eliminated on its boundary. At the same time the role of the process of vertical mixing in the cumulus cloud is of secondary importance [30, 31]. As the estimation of according terms of this system shows for typical values of the meteoparameters, the vertical mixing parameter $\varepsilon \approx 0.1$, and according terms in the system (17) may be neglected. Therefore the considered problem may be referred to the vertical boundary layer type problem (indeed, near the cloud axes the vertical flows are greatly more than horizontal components of wind in it (see also [30, 28])).

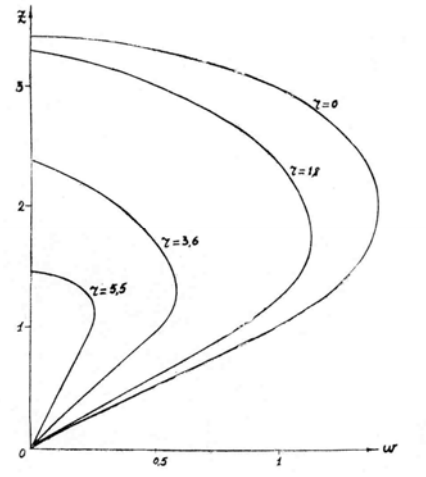

Fig. 9a. Profile of the vertical velocity of air, w, according to [30].

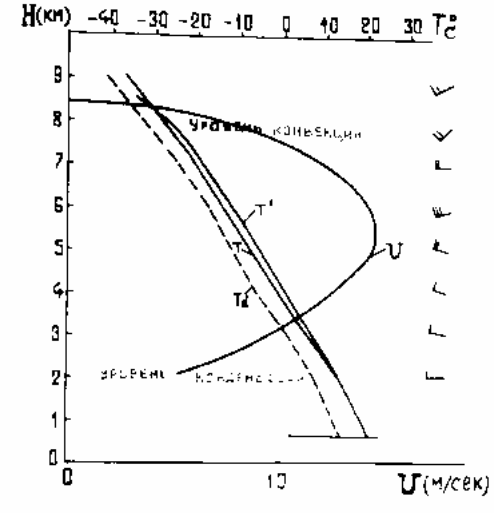

Fig. 9b. Profile of the vertical velocity of air w (here U), according to [29].

It is evident that the values of u and w may be found from this system. After analysis of turbulence conditions for theoretical model of the axisymmetric stationary cumulus cloud, it was established that vertical turbulent mixing is more less than intensive regulate vertical transfer of the air masses. Parameters of the cloud were calculated on the basis of equations system (13). Under the condensation level of the cloud $(1 > z > 0)$ and over it formulas for vertical velocities are, respectively,

$$w = z\exp(-\zeta), \quad \text{and} \quad w = w_0 ch\zeta - zsh\zeta, \qquad (19)$$

where $\zeta = r^2/2n$, $w = 10\,m/s \cdot \bar{w}$, $z = 10^3\,m \cdot \bar{z}$, $r = 316\,m \cdot \bar{r}$, n is an arbitrary constant, the factors before the non-dimensional values signed by a line from above are their scales, respectively.

Fig. 9a shows dependence between the non-dimensional values (without the lines from above) and height, z. The axial value of w is maximal, and equals to

$$w_{\max} = 14.1\ m/s,$$

and to the periphery it slows down to 0, which is in a good accordance with the layer lifting method [12] and the experimental investigations of cumulus cloud dynamics in nature [31].

Fig. 9b shows results of numerical calculations of model convective cloud on the basis of radiosounding and ring chart data of Ruispiri village weather station for the territory of the Alazani Valley (Georgia), 21 June 1969 [29]. It is evident that our and Gutman's model are in accordance with each other.

2.4.2. Thermal in the arbitrary stratified atmosphere ($S = (\theta/T)(\gamma_a - \gamma) = 0$ **)**[12]**.**

Arising above a point heat source owing to turbulent heat conductivity the warm air will begin to ascend forming a thermal.

$$u\frac{\partial u}{\partial r} + w\frac{\partial u}{\partial z} = -\frac{\partial \pi}{\partial r} + \nu_h \frac{\partial}{\partial r}\left(\frac{1}{r}\frac{\partial (ur)}{\partial r}\right), \quad u\frac{\partial w}{\partial r} + w\frac{\partial w}{\partial z} = \frac{\nu_h}{r}\frac{\partial}{\partial r}\left(r\frac{\partial w}{\partial r}\right) + \lambda\vartheta,$$
$$u\frac{\partial \vartheta}{\partial r} + w\frac{\partial \vartheta}{\partial z} = \frac{\nu_h}{r}\frac{\partial}{\partial r}\left(r\frac{\partial \vartheta}{\partial r}\right), \quad \frac{\partial (ur)}{\partial r} + \frac{\partial (wr)}{\partial z} = 0, \qquad (20)$$

with the symmetric boundary layers, the condition of locality of the phenomenon, and the given condition of source heat power, Q, respectively

$$u = \frac{\partial w}{\partial r} = \frac{\partial \vartheta}{\partial r} = 0 \quad \text{at } r = 0, \quad w = \vartheta = \pi = 0 \text{ at } r = \infty; \int_0^\infty w\vartheta r\,dr = Q = const. \qquad (21)$$

Equations system is close relative to u, w, and ϑ. Because perturbation of pressure can be found from first equation after definition of u, w one can conclude that the pressure perturbation plays passive role in the mechanism of a thermal since the latter represents axisymmetric vertical boundary layer.

Along the axis of thermal both the maximal vertical velocity and temperature are, respectively:

$$w\big|_{r=0} = \sqrt{\lambda Q/\nu_h}, \qquad \text{and} \qquad \vartheta\big|_{r=0} = 2Q/(3\nu_h z), \qquad (22)$$

where Q is the heat source capacity, ν_h is the horizontal turbulent coefficient, $\lambda = g/\theta$ is the buoyancy parameter, $\theta = T(1000mb/P)^{AR/c_P}$ is the adiabatic temperature, z is the height above the ground surface.

For typical parameters of surrounding medium we have (in SI: $\lambda \approx 10^{-2}$, Q $\sim (0.1 \div 1)\cdot 10^4$, $\nu_h \approx 1 \div 10$, z $= 10^2$):

$$w\big|_{r=0} \approx 1 \div 2\ m/s, \qquad \vartheta\big|_{r=0} \approx 2 \div 3\,^0C.$$

2.4.3. Spontaneous thermal ($S = (\theta/T)(\gamma_a - \gamma) \neq 0$ **)**[12]**.**

Stationary problem about a spontaneous thermal being in the presence of the energy of the atmosphere vertical instability.

$$u\frac{\partial u}{\partial r}+w\frac{\partial u}{\partial z}=-\frac{\partial \pi}{\partial r}+\nu_h\frac{\partial}{\partial r}\left(\frac{1}{r}\frac{\partial (ur)}{\partial r}\right),\quad u\frac{\partial w}{\partial r}+w\frac{\partial w}{\partial z}=-\frac{\partial \pi}{\partial z}+\frac{\nu_h}{r}\frac{\partial}{\partial r}\left(r\frac{\partial w}{\partial r}\right)+\lambda\vartheta,$$
$$u\frac{\partial \vartheta}{\partial r}+w\frac{\partial \vartheta}{\partial z}+Sw=\frac{\nu_h}{r}\frac{\partial}{\partial r}\left(r\frac{\partial \vartheta}{\partial r}\right),\quad \frac{\partial (ur)}{\partial r}+\frac{\partial (wr)}{\partial z}=0, \tag{23}$$

with the symmetric boundary layers and the condition of locality of the phenomenon

$$u=\frac{\partial w}{\partial r}=\frac{\partial \vartheta}{\partial r}=0 \quad \text{at } r=0,\ \ w=\vartheta=\pi=0 \text{ at } r=\infty. \tag{24}$$

Fig. 10 represents scheme of isolines of current in vertical section of the axisymmetric thermal.

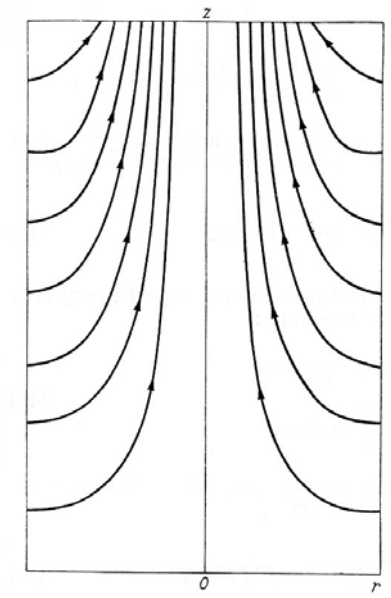

Fig. 10. Current lines in the axial section of the thermal [12].

.

Along the axis of thermal both the maximal vertical velocity and temperature are, respectively:

$$w\big|_{r=0}=\frac{z}{a}\sqrt{-\lambda S},\qquad \text{and}\qquad \vartheta\big|_{r=0}=-\frac{S}{a}z,\qquad a=1.144. \tag{25}$$

For $S=-3\cdot 10^{-3}\ {}^0C/m$, $\nu=10m^2/s$, z = 1 km one may have that

$$w\big|_{r=0}=10\,m/s,\qquad \vartheta\big|_{r=0}=3^0.$$

It is evident that using (22) the thermal's vertical temperature gradient will be near to the dry-adiabatic gradient one.

The radial component of the thermal velocity, u, does not depend on the height and has a maximum equals to

$$u_{\max} \approx -0.5\ m/s, \quad \text{at } r_{\max} = 150\ m.$$

The radial component of the thermal velocity is so small, that its fixation in nature practically is impossible. Attenuation of u at $r \to \infty$ takes place as in case of § 2.4.2, i.e., more slower then w or θ. Using the same values of the thermal parameters, one has that the pressure of air inside of the thermal is less than out of it in surrounding area. Indeed, the disturbed value of air pressure, p', at the center of thermal is

$$p'\big|_{r-0} = -10^{-3}\ mb,$$

Above obtained formulas (19), (22), (25) are exact solutions of according problems. Thus, it is obtained unambiguous non-trivial solution of homogeneous problem, what shows that considered problem is an essentially nonlinear.

2.4.4. Weak thermal vortex rings in the arbitrary stratified atmosphere ($S = 0$) [32]. **Non-stationary axisymmetric case**.

It is naturally to represent that the convection will be axisymmetric relative to the vertical passing through the point in which the heat impulse was supplied.

Input equations are

$$\frac{\partial u}{\partial t} + u\frac{\partial u}{\partial r} + \frac{v}{r}\frac{\partial u}{\partial \varphi} - \frac{v^2}{r} = -\frac{\partial \pi}{\partial r} + \lambda\vartheta\cos\varphi + \nu\left(\Delta u - \frac{2u}{r^2} - \frac{2v\,ctg\,\varphi}{r^2} - \frac{2}{r^2}\frac{\partial v}{\partial \varphi}\right),$$

$$\frac{\partial v}{\partial t} + u\frac{\partial v}{\partial r} + \frac{v}{r}\frac{\partial v}{\partial \varphi} + \frac{uv}{r} = -\frac{1}{r}\frac{\partial \pi}{\partial r} - \lambda\vartheta\sin\varphi + \nu\left(\Delta v - \frac{v}{r^2\sin^2\varphi} + \frac{2}{r^2}\frac{\partial u}{\partial \varphi}\right),$$

$$\frac{\partial \vartheta}{\partial t} + u\frac{\partial \vartheta}{\partial r} + \frac{v}{r}\frac{\partial \vartheta}{\partial \varphi} = \nu\Delta\vartheta, \quad \frac{\partial}{\partial r}(r^2 u\sin\varphi) + \frac{\partial}{\partial \varphi}(rv\sin\varphi) = 0, \tag{28}$$

where $\Delta = \frac{1}{r^2}\frac{\partial}{\partial r}r^2\frac{\partial}{\partial r} + \frac{1}{r^2\sin\varphi}\frac{\partial}{\partial \varphi}\sin\varphi\frac{\partial}{\partial \varphi}$;

the boundary and symmetry conditions are, respectively,

$$u = w = \vartheta = \pi = 0 \text{ at } r \to \infty, \text{ and } v = \frac{\partial u}{\partial \varphi} = \frac{\partial \vartheta}{\partial \varphi} = 0 \text{ at } \varphi = 0 \text{ and } \varphi = 180^0. \tag{29}$$

In general case solution of this non-linear equations system connected with great difficulties. Therefore the author is limited to the case of weak heat impulse when Rayleigh's number analog of convective instability $\alpha = \lambda q/\nu^2 < 1$.

Under condition of conservation of the whole quantity of heat $q = const$, the vertical velocity at the point of origin is

$$w\big|_{r=0} = \frac{\alpha}{12\pi}\sqrt{\frac{\nu}{\pi t}}, \tag{26}$$

where $\lambda = g/\theta$, $\theta = T(1000mb/P)^{AR/c_P}$ is the adiabatic temperature.

In first approximation the point with maximum of the temperature r_0 and the heaving velocity of the formed heat core are equal to, respectively,

$$r_0 \approx \pm(\alpha/12\pi)(\nu t/\pi)^{1/2}\ ,\ \text{and}\ \ dr_0/dt \approx \pm(\alpha/24\pi)(\nu/\pi t)\,. \qquad (27)$$

Obtained solution has asymptotic character and makes sense at sufficiently great values of t. Using $\alpha \sim 1$, $\nu = 1 \div 10\, m/s^2$, from (27) we have

$$r_0 \approx 1m\,, \qquad t = 4\cdot 10^2 s\ ; \qquad dr_0/dt \approx 0.125\ cm/s\,,\ w\big|_{r=0} = 0.25 cm/s\,,$$

$$r_0 \approx 100m\,, \qquad t = 4\cdot 10^3\ s\ ; \qquad dr_0/dt \approx 1.25 cm/s\,,\ w\big|_{r=0} = 2.5 cm/s\,.$$

2.4.5. Automodel solution for a plane problem. **Non-stationary case** [33].

Results of § 2.4.4 show that provided a heat impulse is weak the problem will be linear and solvable analytically. In general case it is necessary to use numerical computing. Because of increasing of the range involved by motion the author overcomes this complication by means of enlarging co-ordinates application.

Input equations are

$$\frac{\partial u}{\partial t} + u\frac{\partial u}{\partial x} + w\frac{\partial u}{\partial z} = -\frac{\partial \pi}{\partial x} + \nu(t)\Delta u\,, \quad \frac{\partial w}{\partial t} + u\frac{\partial w}{\partial x} + w\frac{\partial w}{\partial z} = -\frac{\partial \pi}{\partial z} + \lambda\vartheta + \nu(t)\Delta w\,,$$
$$\frac{\partial \vartheta}{\partial t} + u\frac{\partial \vartheta}{\partial x} + w\frac{\partial \vartheta}{\partial z} = \nu(t)\Delta\vartheta\,, \qquad \frac{\partial u}{\partial x} + \frac{\partial w}{\partial z} = 0\,,\ \ \Delta = \frac{\partial^2}{\partial x^2} + \frac{\partial^2}{\partial z^2}\,; \qquad (28)$$

the boundary conditions,

$$u = \frac{\partial w}{\partial x} = \frac{\partial \vartheta}{\partial x} = 0 \quad \text{at}\ x = 0\,,\ \ u = w = \vartheta = 0\ \text{at}\ x,\ z \to \infty,\ . \qquad (29)$$

the initial conditions, and symmetry and anti-symmetry conditions, respectively,

$$u = w = 0\,,\ \vartheta = \vartheta_0(x,z)\ \ \text{at}\ t = t_0 > 0\,;\ \text{and}\ \vartheta_0(x,z) = \vartheta_0(-x,z) = -\vartheta_0(x,-z)\,. \qquad (30)$$

Using results of analytical and numerical calculations for current lines and temperature isolines represented in figures of [33] we can crude estimate the vertical arising velocity of the hot core (plume): $z = a_w(9\lambda Q/4)^{1/3} t^{2/3}$,

$$w = (2/3)a_w(9\lambda Q/4)^{1/3} t^{-1/3}\,,. \qquad (31)$$

choosing $\overline{a_w} \approx 0.3$, $\lambda = g/\theta \approx 0.03$, $Q = (4 \div 40)\, kJ/s$, $\Delta z = 0.3\cdot\left(9\lambda Q/4\right)^{1/3} t^{2/3}$, we have:

$$w \approx\ 4 \div 6\ \text{m/s}.$$

The solution in every case approaches to the steady-state conditions. It is necessary to note that in case of § 2.4.4 the vortex don't emerge because of the problem proximity. In present case as above generates a pair of symmetric linear vortexes (not ring). They gradually move away from the point of origin and with each other and rise upward, involving in motion more and more new portions of air. Lower part of warmed-up region is converged shaping of stalk, conduit which finally breaks. The hot core (as a plume) rises upward and move away from the z-axis. In stable regime together with the initial vortex arises a small inverse vortex. Because of difficulties of comparison of theoretical results with observations in nature, the author compared those with the laboratory experiments. The solution in every instances approaches to a stationary regime.

2.4.6. Mountain meteorology.

In [34] for the case of steep and large-amplitude topography (mountainous terrain) was shown that even a gentle hill can lead to highly complex phenomena such as separation zones and lee-side turbulent wakes. With increasing obstacle height and steepness, these effects can assume considerable dimensions. The convective velocity scale, w_*, equals to

$$w_* = [(g/\overline{\theta_0})\overline{w'\theta_0'}z_i]^{1/3}, \qquad (32)$$

where z_i is the mixed-layer height, $\overline{w'\theta_0'}$ is the surface turbulent kinematic heat flux, and $\overline{\theta_0}$ is the surface potential temperature, – are the characteristic variables. Measurements and calculations give following result on the value of the convective velocity scale (z = 300÷700 m)

$$w_* \approx 1.5\ m/s\ .$$

Radar observations give a direct estimate of the root mean square (r.m.s.) turbulent velocities (in the vertical direction) in air parcels passing overhead of the radar site, and their temporal variability at that single location.

2.4.7. Mesoscale convective system observed from satellite [15].

In conclusion of this section, we provide the impressive picture of thermals ensemble observed from satellite in infrared rays (Fig. 11).

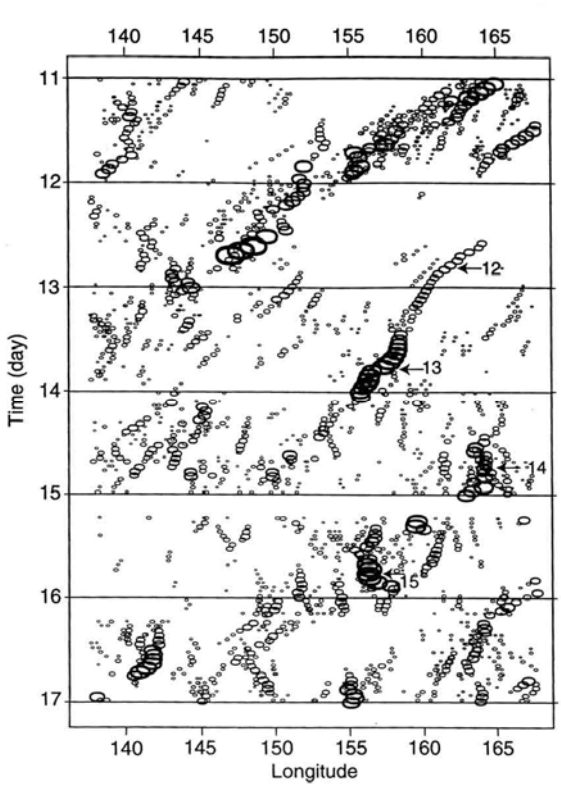

Fig. 11. Mesoscale convective systems observed from satellite [35, 15]

It is well seen a wave in the mesoscale convective system. Convective clouds have long been viewed as forming from buoyant bubbles or "parcels" of air emanating from the planetary boundary layer. While this view certainly describes nearly all smaller convective clouds, the organized vertical circulation in a large, mature MCS takes on a different type of

organization, which is better described by layer lifting than parcel concepts [15]. It is interesting to consider this picture as an hierarchy of mesoscale vortexes in a turbulent medium [36].

3.1. The middle atmosphere and lower thermosphere.

At that levels a source of heat is the Joule heating caused by the high-latitude electrojets during magnetic storms. The Joule heating rate, Q, may be calculated by means of the following formulas [37]:

$$Q = const\frac{\Sigma_P}{\Sigma_H^2}\cdot(\Delta H)^2 \quad \text{or} \quad Q_J = E_h^2\cdot\Sigma_P, \tag{20}$$

where $Q/(\Delta H)^2$ varies by a factor of 100, H is the geomagnetic field, Σ_P and Σ_H are the height-integrated Pedersen and Hall conductivities, respectively, Q_J is the height-integrated Joule heating rate, E_H is the horizontal electric field. The maximal value of the heating rate is about

$$Q_J^{\max} = 3\div 40\ mW\,m^{-2}. \tag{20a}$$

Convective motion in this region of upper atmosphere can be generated as a result of that heating, which may be observed and calculated, too.

Respective upward wind speed, w, is [38]:

$$w = \varepsilon\left(c_p\frac{\partial T}{\partial z} + g\right)^{-1}, \tag{21}$$

where ε is the heating rate and g the acceleration due to gravity.

More detailed [39], when a unit mass of air moves vertically with speed w and, is heated with speed

$$\frac{dQ}{dt} = \rho c_p\frac{dT}{dz}w, \tag{22}$$

and executes mechanical work with a speed

$$-\frac{dP}{dt} = \rho g w, \tag{23}$$

here it was used the barometric law $dP/dz = -\rho g$. Then for full energy obtained by the unit mass of air $E = \frac{dQ}{dt} - \frac{dP}{dt}$ and the vertical velocity w are equals to, respectively,

$$E = \rho\left(c_p\frac{dT}{dz} + g\right)w, \qquad w = \frac{E}{\rho}\left(c_p\frac{dT}{dz} + g\right)^{-1}.$$

In isothermal atmosphere $dT/dz = 0$, $E = \rho g w$, or $w = E/\rho g$.

The energy budget estimated on the basis of the various measurements performed during the campaign showed two specific altitude levels: 120-140 km, where Joule heating dominates, and 90-110 km, where precipitating particles dissipate their energy. Joule heating during moderate to strong geomagnetic disturbances was found to be considerably larger than particle heating, if mean values are compared, very much larger than solar EUV and UV heating rates. Values of 100 and $280\,K\,d^{-1}$ were obtained in moderate to strong geomagnetic disturbances. To determine the actual temperature increase of the air one has to multiply these numbers by the time period during which the heating effectively acts on the air. This is either

the duration of geomagnetic disturbance of the residence time of the air within the auroral oval. It was found that wind speeds were rather higher and hence residence times were of the order of 1-3 h (the rocket temperature measurements of the air give an effective residence time ~ 1 h).

Using (21) one can obtain, that an otherwise unbalanced heating rate ε = 100K h^{-1} yields a vertical velocity

$$w = 1.3\ m s^{-1}, \qquad (25)$$

if a typical temperature gradient $\partial T / \partial z$=12K km^{-1} is used. The Joule heating rates observed during MAP experiment thus should lead to vertical wind speeds of a few meters per second in the lower thermosphere. As we above saw about such order of values of velocities are observed at the troposphere levels (1). The main part of the absorption occurs below 100 km and is expected to be sensitive to precipitating electrons above a few tens of keV. Observations showed that during 24 h the ratio of heating rates: Joule heating/absorption changes from 1.3 to 3.6, and Joule heating/emission from 2.2 to 17.3. Thus, the Joule heating is responsible for convection, as it was mentioned, at the specific altitude levels 120-140 km [37].
Besides, winds changing are apparently very important.

3.2. Vertical circulation in the upper atmosphere during magnetic storm.
In global scale convection, vertically moved air masses are formed circle in the meridional section as is shown in Fig. 12 and considered, for example, in the articles [39-46].

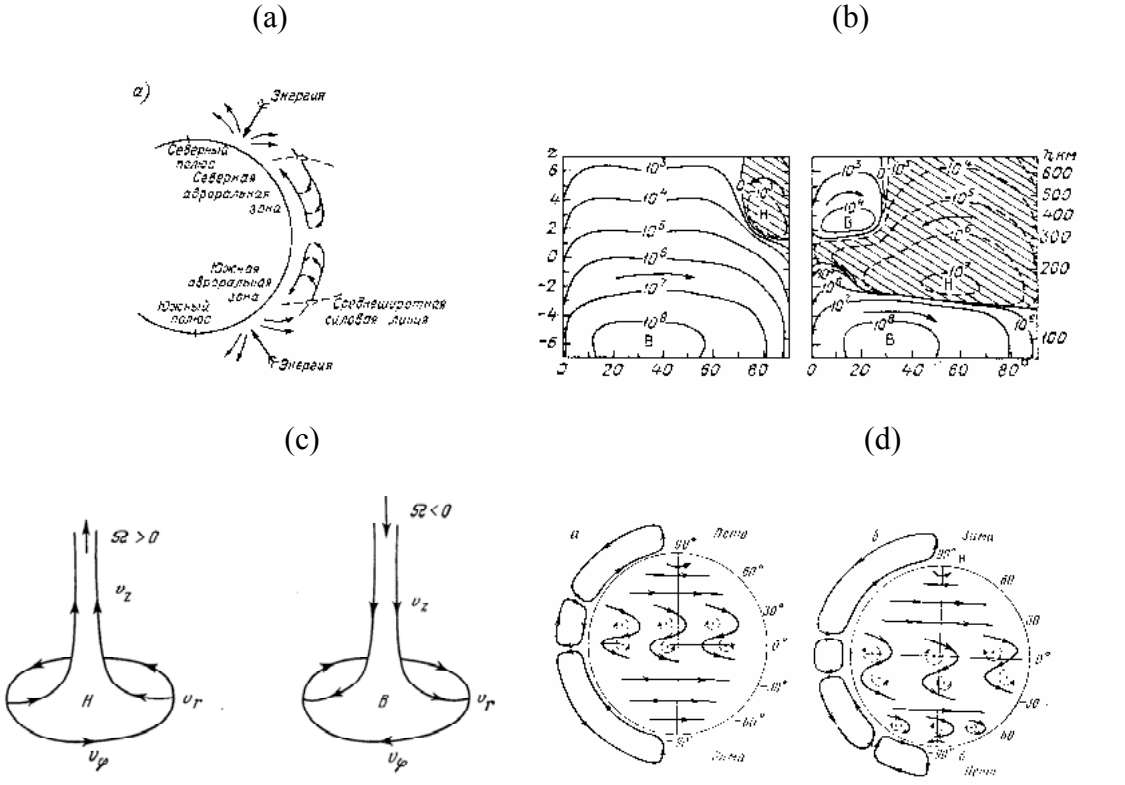

Fig. 12. Vertical circulation cells in the upper atmosphere according to Rishbeth [39] – (a), Dickinson et al. [40, 41] – (b); up-and-down motion of air in the pair of vortexes – (c) and global circulation of the ionosphere – (d) according to [42, 43].

Theoretical models [42-44] describe large-scale picture of general circulation of ionosphere by means of simplified equations – conditions of equilibrium of pressure gradient

$\vec{G} = \rho^{-1}\nabla P$, Coriolis $2[\vec{v}\cdot\vec{\omega}]$ and electromagnetic forces $-\lambda\vec{v}_\perp$ and $2[\vec{v}\cdot\vec{\Omega}]$, $\vec{v}_\perp \approx \vec{v} = \vec{u}$, we have

$$\vec{u} = \frac{\lambda}{\lambda^2 + 4\Omega_1^2}\vec{G} + \frac{2\Omega_1}{\lambda^2 + 4\Omega_1^2}[\vec{G}\cdot\vec{k}]\,. \qquad (26)$$

where the first item is a velocity of wind directed along the pressure gradient $\vec{G}$ (from great values of pressure to less ones), and the second item – along the isobars, λ and Ω_1 are the pure magnetic anisotropic friction and generalized gyroscopic coefficients, respectively; P and ρ are the gas pressure and density, respectively, $\vec{k}$ is a unit vector of the z-axis. Therefore, knowing only the pressure field in the upper atmosphere (especially in the F-region) we can determine a distribution of the wind velocities there; in particular, vertical velocity of ionosphere's gas. For elements of general circulation we obtain simple formulas for vertical component of vortex, two-dimensional divergence, and vertical component of the wind velocity,

$$\Omega_z = \frac{2\Omega_1}{\lambda^2 + 4\Omega_1^2}\frac{1}{\rho}\Delta P, \qquad Div\,\vec{v} = -\frac{\lambda}{\lambda^2 + 4\Omega_1^2}\frac{1}{\rho}\Delta P,$$

$$w = \frac{\lambda}{\lambda^2 + 4\Omega_1^2}\int_0^z \frac{\Delta P}{\rho}dz\,. \qquad (27)$$

At z ≈ 300 km, as evident from Fig. 13, on the latitudes $\varphi = 30^0\,N$ and $-20^0\,S$, in winter, convergence of horizontal air currents must both reduce to vertical motion and form meridional

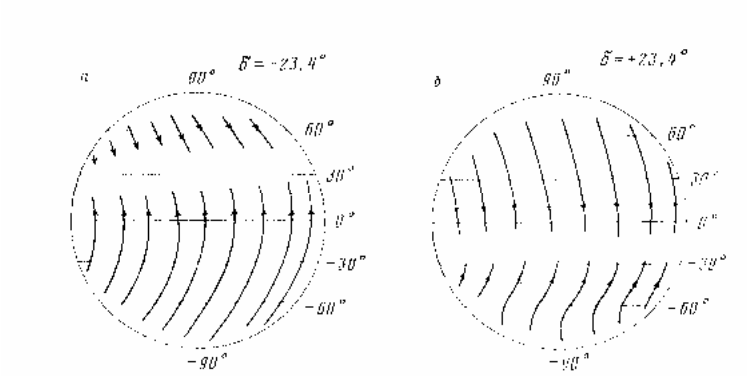

Fig. 13. Picture of midnight winds in the ionosphere F-region at z = 300 km [43].

circular cells in the ionosphere. Obtained in [42] horizontal system of vortexes at the heights z ≤ 200 km near these latitudes give grounds for putting forward the vortical mechanism of vertical
motions generation at the ionosphere levels. Vortical structure of wind pattern at mentioned latitudes supporting from below by forcing of the wind system is broken and at z > 300 km to 400 km there is tendency to the potentiality of the wind (vortex exists, though too little). At z~500 km this peculiarity vanishes, therefore vertical component of velocity vanishes, too, and thereby, the upper boundary of vertical meridional cell is defined.

In spherical coordinates system for wind velocities components at z =,300 km we have [43]:

$$u \approx -\frac{1}{\rho\lambda_0 r\sin\theta}\frac{\partial P}{\partial\psi}, \qquad v \approx \frac{1}{\rho\lambda r}\frac{\partial P}{\partial\theta}.$$

$$w \approx \frac{1}{R}\frac{c^2}{\overline{\sigma}_\perp H_0^2 \cos^2\chi}\frac{\partial^2 P}{\partial\theta^2}\Delta z\,, \qquad (28)$$

where R is the Earth radius, θ is the colatitude, ψ is the longitude, χ is the angle between a vertical line and geomagnetic field, $\overline{\sigma}_\perp$ is the transversal conductivity of ionospheric plasma, H_0 is the absolute value of the geomagnetic field, c is the velocity of light.

On the basis of the ionosphere and neutral atmosphere models (Fatkullin et al., 1981; Jacchia, 1971) [43], at z = 300 km were calculated the parameters of the ionosphere:

$$\mathrm{r} = \mathrm{R} + \mathrm{z},\ \mathrm{R} \approx 6.4\cdot 10^8\ \mathrm{cm},\ H_0 = 0.5\,Gs\,,\ \cos^2\chi = 0.7,\ \overline{\sigma}_\perp c^{-2} = 2\cdot 10^{-16}\,CGSM\,,$$
$$\frac{\partial^2 P}{\partial\theta^2} = 0.4\cdot 10^{-12}\,g(cm\cdot s^2\cdot deg)^{-1},\ \Delta z = 5\cdot 10^6\ \mathrm{cm}. \qquad (29)$$

Using equations (28) and the equation of discontinuity for vertical velocity, in β-plane approximation, for middle-latitudinal ionosphere the velocity of ascending air

$$w \approx 1\ m\cdot s^{-1}\,. \qquad (30)$$

4. Conclusion.

Thus, carried out original analytical and numerical investigations showed that large-scale eddy regions and zones of divergence and convergence responsible to existence of three-dimensional motions of air in the neutral atmosphere and in the ionosphere.

References

[1] Rumford C. Of the propagation of heat in fluids. Complete Works, American Academy of Arts and Sciences, 1870, v. 1, p. 239.

[2] Thomson J. T. On a changing tesselated structure in certain liquids. Proc. Glasgow Philos. Soc, 1881, v. 2.

[3] Bénard M. Les tourbillons cellularies dans une nappe liquide. Revue General de Sciences, 1900, v. 12, pp. 1261-1309.

[4] Bénard M. Les tourbillons cellularies dans une nappe liquide transportant de la chaleur par convection en regime permanent. Ann. de Chimie et de Physique. 1901, v. 23, p. 62.

[5] Rayleigh O. M. On convection currents in a horizontal layer of fluid when the higher temperature is on the under side. Philos. Mag. and J. Sci., 1916, v. 32, N192, pp. 529-546.

[6] Dubuk A. F. Convective motions in atmosphere. Meteorologia i Gidrologia, 1946, N 6.

[7] Priestley C. H. B. Buoyant motion in a turbulent environment. Austral. J. Physics, 1953, v. 6, N 5.

[8] Priestley C. H. B. Convection from earth's surface. Proc. Roy. Soc., 1953, v. 238, N1214. .

[9] Malkus J. S. Some results of a trade-cumulus cloud investigation. J. Meteorol., 1954, v. 11, N 3.

[10] Stommel H., Arons A., Blanchard D. An oceanographical curiosity: the perpetual salt fountain. Deep-Sea Res., 1956, v. 3, N 2, pp. 152-153.

[11] Chandrasekhar S. Hydrodynamic and hydromagnetic stability. Clarendon Press, Oxford, England, 1961, 652 p.

[12] Gutman L. N. Introduction to the nonlinear theory of mesometeorological processes. L.: Gidrometeoizdat, 1969, 295 p.

[13] Joseph D. D. Stability of fluid motions. Springer-Verlag, Berlin-Heidelberg-New York, 1976 ; M: Mir, 1981, 638 p.

[14] Golitsyn G. S. Energy of convection. Non-linear waves: Stochasticity and Turbulence. Gorky: AN SSSR, IPF, 1980, pp. 131-139.

[15] Houze R. A. Jr. Mesoscale convective systems. Reviews of Geophysics, 2004, v. 42, RG4001, pp. 1-29.
[16] Jellinek A. M., Manga M. Links between long-lived hot spots, mantle plumes, D″, and plate tectonics. Reviews of Geophysics, 2004, v. 42, RG3002, pp. 1-35.
[17] Dynamical meteorology, (Eds. Izvekov B. I.and Kochin N. E.). GidroLenredizdat TsEGMS, 1935, v. 1.
[18] Sulakvelidze G. K., Sulakvelidze Ya. G. Thermodynamics of troposphere. Part I. Tbilisi, TSU, 1980, 294 p.
[19] Shishkin N. S. Calculations of vertical flows by layer method. Trudy GGO, v. 57, 1959.
[20] Shishkin N. S. To the calculation of the velocity of the convective clouds vertical growth. Trudy GGO, v. 104, 1960.
[21] Orjonikidze A. A. To the question of estimation of the atmosphere thermal instability. Proceedings of the All-Union Conference on the Active Influence upon the Hail Processes.
Tbilisi, Institute of Geophysics, Georgian Academy of Sciences, 1964, pp. 262-270.
[22] Bukhnikashvili A. V., Gaivoronsky I. I., Kartsivadze A. I., Kiziria B. I., Okujava A. M., Orjonikidze A. A., Sarkisova L. S., Seregin Yu. A. Active influence upon hail processes
and results of experiments provided in the Alazani Valley. Proceedings of the All-Union Conference on the Active Influence upon the Hail Processes. Tbilisi, Institute of Geophysics, Georgian Academy of Sciences, 1964, pp. 281-324.
[23] Kartsivadze A. I., Makharadze G. M., Orjonikidze A. A. Experimental study of vertical motions in convective clouds. Transactions of Institute of Geophysics of Georgian SSR Academy Sci., 1972, v. XXVIII, pp. 196-209.
[24] Eidinova G. Z. To the problem of cumulus clouds tops growth velocity. Transactions of Institute of Geophysics of Georgian SSR Academy Sci., 1972, v. XXVIII, pp. 145-154.
[25] Balabuev A. G. Some results of convective clouds photogrammetric observations in the Alazany Valley. Transactions of Institute of Geophysics of Georgian SSR Academy Sci., 1967, v. XXV, N 1, pp. 25-34.
[26] Belinsky V. A. Dynamical meteorology. M.–L.: OGIZ GITTL, 1948, 703 p.
[27] Bryan G. H., Fritsch J. M. On the existence of the convective rolls in the convective region of squall lines. 10th Conference on Mesoscale Processes, Am. Meteorol. Soc., Portland, Oreg., 23-27 June, 2003.
[28] Kachurin L. G. Physical principles of influencing at the atmospheric processes. L.: Gidrometeoizdat, 1990, 463 p.
[29] Gvelesiani A. I. Some aspects of the hail particles evolution. Ph.D. Thesis, Leningrad: LGMI, 1970, 211 p.
[30] Gutman L. N. Approximate nonlinear theory of a stationary cumulus cloud. Proceedings of the All-Union Conference on the Active Influence upon the Hail Processes.
Tbilisi, Institute of Geophysics, Georgian Academy of Sciences, 1964, pp. 132-149.
[31] Ogura Y. The evolution of a moist convective element in a shallow, conditionally unstable atmosphere: A numerical calculation. J. Atmos. Sci., 1963, v. 20, N5, pp. 407-424.
[32] Morton B. R. Weak thermal vortex rings. J. Fluid Mech., 1960, v. 9, pp. 107-118.
[33] Lilly D. K. Numerical solutions for the shape-preserving two-dimensional thermal convection element. J. Atm. Sci., 1956, v. 21, N 1.
[34] Weigel A. P., F. K. Chow, M. W. Rotach. On the nature of turbulent kinetic energy in a steep and narrow Alpine valley. Boundary-Layer Meteorol. DOI 10.1007/s10546-006-9142-
9. Springer Science-Business Media B.V. 2006.
[35] Chen S. S., Hauze R. A. Jr., Mapes B. E. Multiscale variability of deep convection in

relation to large-scale circulation in TOGA COARE. J. Atmos.Sci., 1996, v. 53, pp. 1380-1409.
[36] Gvelesiani A. I. On the hierarchy of mesoscale vortexes in the turbulent medium. J. Georgian Geophys. Soc., 2006, v. 11B, pp. 3-11.
[37] Baumjohann W., Gustafsson G., Nilsen E., Ranta H., Evans D. S. Latitude-integrated Joule and particle heating rates during the Energy Budget Campaign 1980. J. Atmos. Terr. Phys., 1985, v. 1-3, pp. 27-39.
[38] Offermann D. The Energy Budget Campaign 1980: introductory review. J. Atmos. Terr. Phys., 1985, v. 1-3, pp. 1-26.
[39] Hargreaves J. K. The upper atmosphere and solar-terrestrial relations. An introduction to the aerospace environment. Van Nostrand Reinhold Company, New York-Cincinnati-Toronto-London-Melbourne. 1977 (1982, Russian), 352 p.
[40] Dickinson R. E., Ridley E. C., Roble R. G. Meridional circulation in the thermosphere. I. J. Atmos. Sci., 1975, v. 32, N 9, pp. 1737-1754.
[41] Dickinson R. E., Ridley E. C., Roble R. G. Meridional circulation in the thermosphere. II. J. Atmos. Sci., 1977, v. 34, N 1, pp. 176-192.
[42] Khantadze A. G., Gvelesiani A. I. Influence of ionosphere plasma on the general circulation of high atmosphere. I. Geomagnetism i Aeronomia, 1981, v. 21, N6, pp. 988-992; 1982, v. 22, N1, pp. 66-69.
[43] Gvelesiani A. I. On the meridional winds in the ionosphere. Geomagnetism i Aeronomia, 1985, v. 25, N1, pp. 58 – 62.
[44] Gvelesiani A. On the energy budget of the mesosphere and lower thermosphere. J. Georgian Geophys. Soc., 2002, v. 7B, 46 - 51.
[45] Gvelesiani A. I. To the problem of the upper atmosphere turbulence. J. Georgian Geophys. Soc., 2008, v.12B, pp. 52-75.

(Received in final form 25 November 2009)

О конвективных движениях в различных слоях атмосферы

Анзор И. Гвелесиани

С единой точки зрения рассматриваются результаты теоретических и экспериментальных исследований медленных мезомасштабных конвективных движений в атмосфере. Учтена специфика режимов рассматриваемых сред при определении условий возникновения конвекции и нахождении аналитических формул для вертикальной скорости восходящего потока воздуха. Проведённые аналитические и численные исследования показывают, что в ионосфере должны существовать крупномасштабные вихревые образования и зоны схождения и расхождения ветров, ответственные за трёхмерность движений воздуха.

კონვექციური მოძრაობების შესახებ ატმოსფეროს სხვადასხვა ფენაში

ანზორ ი. გველესიანი

რეზიუმე

ერთი მთლიანი თვალსაზრისით განხილულია ატმოსფეროში ნელი კონვექციური მეზომასშტაბური მოძრაობების თეორიული და ექსპერიმენტული

შესწავლის შედეგები. კონვექციის წარმოშობის პირობებისა და აღმავალი თერმიკის ვერტიკალური სიჩქარის ანალიზური ფორმულების განსაზღვრისას გათვალისწინებულია განხილულ გარემოთა რეჟიმების სპეციფიკა. ჩატარებული ანალიზური და რიცხვითი გამოკვლევები გვიჩვენებს, რომ იონოსფეროში უნდა არსებობდნენ დიდმასშტაბიანი გრიგალური წარმონაქმნები და ქარის დივერგენციის და კონვერგენციის ზონები, რომელთა ერთობლიობა პასუხისმგებელია ჰაერის მოძრაობის სამგანზომილეობაზე.